Molecular Biology of the Cell
Vol. 17, 5198–5210, December 2006

Staphylococcus aureus Fibronectin Binding Protein-A Induces Motile Attachment Sites and Complex Actin Remodeling in Living Endothelial Cells[D] [V]

Andreas Schröder,*† Barbara Schröder,‡§ Bernhard Roppenser,* Stefan Linder,‡ Bhanu Sinha,‖ Reinhard Fässler,¶ and Martin Aepfelbacher*

*Institut für Medizinische Mikrobiologie, Virologie und Hygiene, Universitätsklinikum Hamburg-Eppendorf, 20246 Hamburg, Germany; †Max von Pettenkofer-Institut, Ludwig-Maximilians-Universität München, 80336 Munich, Germany; ‡Institut für Prophylaxe der Kreislaufkrankheiten, Ludwig-Maximilians-Universität München, 80336 Munich, Germany; ‖Institut für Medizinische Mikrobiologie, Universitätsklinikum Münster, 48149 Münster, Germany; and ¶Max-Planck-Institut für Biochemie, Abteilung für Molekulare Medizin, 82152 Martinsried, Germany

Submitted May 31, 2006; Revised September 14, 2006; Accepted September 26, 2006
Monitoring Editor: Ralph Isberg

***Staphylococcus aureus* fibronectin binding protein-A (FnBPA) stimulates $\alpha5\beta1$-integrin signaling and actin rearrangements in host cells. This eventually leads to invasion of the staphylococci and their targeting to lysosomes. Using live cell imaging, we found that FnBPA-expressing staphylococci induce formation of fibrillar adhesion-like attachment sites and translocate together with them on the surface of human endothelial cells (velocity ~50 μm/h). The translocating bacteria recruited cellular actin and Rab5 in a cyclic and alternating manner, suggesting unsuccessful attempts of phagocytosis by the endothelial cells. Translocation, actin recruitment, and eventual invasion of the staphylococci was regulated by the fibrillar adhesion protein tensin. The staphylococci also regularly produced Neural Wiskott-Aldrich syndrome protein-controlled actin comet tails that further propelled them on the cell surface (velocity up to 1000 μm/h). Thus, *S. aureus* FnBPA produces attachment sites that promote bacterial movements but subvert actin- and Rab5 reorganization during invasion. This may constitute a novel strategy of *S. aureus* to postpone invasion until its toxins become effective.**

INTRODUCTION

For the purpose of tissue penetration, invasion of the vasculature, and dissemination via the bloodstream, the bacterial pathogen *S. aureus* produces a plethora of virulence factors, including teichoic acids, exotoxins, and adhesins (Lowy, 1998). Collagen-binding Cna, fibrinogen-binding clumping factor-A and -B, and fibronectin binding protein-A and -B (FnBPA and -B) are among the most important adhesins of *S. aureus* (Jonsson *et al.*, 1991; Patti *et al.*, 1992; McDevitt *et al.*, 1994; Menzies, 2003). Although *S. aureus* is considered an extracellular pathogen, it has been well documented that its fibronectin (Fn) binding adhesins FnBPA and -B also mediate bacterial invasion of cells (Sinha *et al.*, 1999, 2000; Fowler *et al.*, 2000; Massey *et al.*, 2001). However, after invasion of human endothelial cells and keratinocytes, the majority of the internalized staphylococci are effectively eliminated by lysosomal effector mechanisms (Krut *et al.*, 2003; Schröder *et al.*, 2006).

In a recent animal study, staphylococci were shown to preferably adhere to capillaries and postcapillary venules after intraarterial injection (Laschke *et al.*, 2005). Most staphylococci (>99%) disappeared from the blood vessels within 20 min, suggesting internalization by the endothelium. An animal endocarditis model demonstrated that expression of FnBPA conferred on staphylococci and lactococci the capability to infect heart valves, resulting in invasion of the valvular endothelium (Que *et al.*, 2005). Hence, the adhesins FnBPA and -B crucially determine interaction of *S. aureus* with endothelial cells in vivo and in vitro.

FnBPs contain multiple modules, each of which can bind to a stretch of type I (F1) repeats at the N terminus of Fn (Massey *et al.*, 2001; Schwarz-Linek *et al.*, 2004). Presumably, FnBPs are thereby capable of associating with several Fn molecules at once (Schwarz-Linek *et al.*, 2004). Furthermore, the FnBP binding site is located at some distance from the central integrin binding RGD motif in Fn. Therefore, Fn can form a bridge between FnBPs and integrins (Sinha *et al.*, 1999; Fowler *et al.*, 2000). Apparently through these features, FnBPs are capable of inducing integrin clustering and signaling in cells. This leads to invasion of staphylococci via src tyrosine kinase activation and reorganization of the actin cytoskeleton (Agerer *et al.*, 2003; Fowler *et al.*, 2003).

Physiological clustering of integrins by extracellular cues causes formation of adhesion structures that differ by morphology, molecular composition, and spatiotemporal dy-

This article was published online ahead of print in *MBC in Press* (http://www.molbiolcell.org/cgi/doi/10.1091/mbc.E06–05–0463) on October 4, 2006.

[D] [V] The online version of this article contains supplemental material at *MBC Online* (http://www.molbiolcell.org).

§ Present address: Center for Basic Research in Digestive Diseases and Department of Biochemistry and Molecular Biology, Mayo Clinic, Rochester, MN 55905.

Address correspondence to: Martin Aepfelbacher (m.aepfelbacher@uke.uni-hamburg.de).

namics. Focal adhesions are tight clusters of cytoskeletal and signaling proteins, including focal adhesion kinase (FAK), vinculin, paxillin, talin, and tensin. These proteins cooperatively organize the association of actin stress fibers with the cytoplasmic domains of integrins (Zamir and Geiger, 2001; Brakebusch and Fässler, 2003; DeMali *et al*., 2003). It has been proposed that fibrillar adhesions develop by translocation of Fn-ligated $\alpha5\beta1$ integrins out of focal adhesions. Fibrillar adhesions have an elongated or beaded morphology and contain tensin, but they are devoid of most other focal adhesion components. The current notion is that fibrillar adhesions stretch extracellular Fn molecules and thereby perpetuate Fn fibrillogenesis (Pankov *et al*., 2000; Zamir *et al*., 2000; Zamir and Geiger, 2001; Danen *et al*., 2002).

So far, the molecular mechanisms controlling adhesion and internalization of staphylococci were visualized mainly in fixed cells. Naturally, this could only provide snapshots of highly dynamic processes. Based mainly on live cell imaging data we report here that the staphylococcal adhesin FnBPA triggers formation of fibrillar adhesion-like attachment sites that encompass the bacteria and mediate their centripetal translocation on the cell surface. The translocating staphylococci induced multiple consecutive actin cups as well as actin comet tails propelling the bacteria on the cell surface. Movements, actin reorganization and final internalization of the bacteria were regulated by the fibrillar adhesion protein tensin.

We propose that FnBPA-stimulated integrin signaling promotes bacterial motility on the endothelial cell surface but retards bacterial invasion. Thus, disturbance of the cellular phagocytic machinery may determine the outcome of endothelium infection by *S. aureus* in disease states such as sepsis or endocarditis.

MATERIALS AND METHODS

Bacterial Strains and Culture Conditions

Escherichia coli HB101 strain expressing Invasin of *Yersinia enterocolitica* named *Invasin-E. coli* was cultured in LB medium as described previously (Schulte *et al*., 1998). *S. aureus* DU 5883(pFnBA4) named *FnBPA-S. aureus* expressing full-length FnBPA (Greene *et al*., 1995) was cultured in LB medium containing 20 μg/ml tetracycline, 5 μg/ml erythromycin, and 20 μg/ml chloramphenicol. *S. carnosus* TM300(pFNBA4) named *FnBPA-S. carnosus* heterologously expressing full-length FnBPA from *S. aureus* (Sinha *et al*., 2000) was cultured in LB medium containing 20 μg/ml chloramphenicol. For infection assays, overnight cultures were diluted 1:10 in LB medium and grown to an OD_{600} of 0.8. Subsequently, strains were centrifuged and bacterial pellets were carefully resuspended in sterile phosphate-buffered saline (PBS), pH 7.4. For infection assays, the volume of PBS containing bacteria for an infection ratio (multiplicity of infection) of 100 bacteria per cell was added to the cell culture medium.

Cell Culture and Infection Assays

Isolation of human umbilical vein endothelial cells (HUVECs) was performed as described previously (Essler *et al*., 2003). Cells were cultured in endothelial cell growth medium (Promocell, Heidelberg, Germany) containing 2% fetal calf serum at 37°C, 5% CO_2, and 90% humidity. For infection assays, HUVECs (2×10^4 cells) were seeded onto gelatin-coated glass coverslips (12 mm; Hartenstein, Würzburg, Germany) kept in eight-well plates (Nalge Nunc International, Rochester, NY) 1 d before the experiment. Thirty minutes before adding the bacteria, the medium was replaced by antibiotic-free medium. In some experiments cells were centrifuged at 44*g* for 5 min after adding bacteria to allow simultaneous attachment of the bacteria. For live cell imaging, HUVECs (2×10^4 cells) were seeded onto glass-bottomed dishes (MatTek, Ashland, MA) 1 d before the experiment. The medium was replaced by antibiotic- and phenol red-free medium 30 min before start of imaging. Bacteria were pipetted in appropriate amounts to the medium and sedimented onto the cells.

Floxed Fn cells were isolated from mice carrying a conditional Fn allele, immortalized, and cloned. Subsequently, the Fn alleles were deleted by adenoviral *Cre* transduction ($Fn^{-/-}$ cells). The cells were grown in DMEM supplemented with 10% fetal calf serum (FCS) or alternatively, in serum replacement medium (Sigma Aldrich, Taufkirchen, Germany).

Transfection and Plasmids

HUVECs were transfected with the Amaxa nucleofection system (Amaxa, Cologne, Germany) applying the standard protocol as specified by the manufacturer. The green fluorescent protein (GFP) fusion vector GFP-C1 and GFP-actin construct were obtained commercially (BD Clontech, Heidelberg, Germany). Constructs encoding for chicken GFP-tensin (Chuang *et al*., 1995) and chicken GFP-tensin AH2 (corresponding to residues 659-762) were gifts of Dr. Shin Lin (University of California, Irvine, Irvine, CA), GFP-Arp3 was kindly provided by Dr. Dorothy Schafer (University of Virginia, Charlottesville, VA), GFP-neural-Wiskott-Aldrich syndrome (N-WASp) was donated by Dr. Silvia Lommel (Helmholtz Centre for Infection Research, Braunschweig, Germany), and GFP-Rab5 was a generous gift of Dr. Craig Roy (Yale University School of Medicine, New Haven, CT). The construct encoding for monomeric red fluorescent protein (mRFP)-actin has been described previously (Osiak *et al*., 2005).

Antibodies and Reagents

Antibodies used for immunofluorescence staining: anti-fibronectin (1:500; BD Transduction Laboratories, Heidelberg, Germany) anti-paxillin (1:200 BD Transduction Laboratories), anti-vinculin (1:50; Sigma Aldrich), anti-pFAK (1:50; BioSource International, Camarillo, CA) and anti-glutathione *S*-transferase (GST) (diluted 1:100; Invitrogen, Leiden, The Netherlands). Inside/outside staining for *S. aureus* was performed with a commercially available antibody against whole bacterial lysate (1:2000; Biodesign International, Saco, ME); for invasin detection, a rabbit polyclonal antiserum was used (1:500; a kind gift of Dr. G. Grassl, Max von Pettenkofer-Institut, University of Munich, Germany). Wiskostatin (Merck Biosciences, Bad Soden, Germany) was used at a final concentration of 2.5 μM.

Expression of GST, GST-Inv397, and GST-FnBPA-Du-D4

Expression and purification of GST and GST-Inv397 was performed as described previously (Wiedemann *et al*., 2001). GST-FnBPA-Du-D4 was expressed according to the same protocol, except that *E. coli* BL21 harboring pGEX-4T-FnBPA-Du-D4 was grown at 37°C, and induction of expression was induced with isopropyl-β-D-thiogalactopyranoside at a final concentration of 1 mM. Purity and identity of GST-Inv397 and GST-FnBPA-Du-D4 fusion proteins were analyzed by SDS-PAGE and Western blot by using goat anti-GST (diluted 1:1000; Molecular Probes, Eugene, OR) and anti-invasin antiserum (diluted 1:5000; see above). Protein concentrations were determined using the BCA protein assay (Pierce Chemical, Rockford, IL). C3-transferase, N17Rac, and N17CDC42 were expressed and purified as GST-fusions as described previously (Wiedemann *et al*., 2001). For microinjection, proteins were dialyzed against buffer (50 mM Tris-HCl, pH 7.5, 150 mM NaCl, and 5 mM $MgCl_2$), concentrated in Centricon or Microcon (Millipore, Billerica, MA), shock frozen, and stored at −80°C. Purity was tested using SDS-PAGE and Coomassie staining.

Coating of Proteins to Latex Beads

About 1×10^9 latex beads (1 μm in diameter, sulfate microspheres; Invitrogen) were washed and resuspended in 1 ml containing 1 mg each of GST, GST-Inv397, or GST-FnBPA-Du-D4. The protein was allowed to adsorb to the beads for 3 h at room temperature. After adding 500 μl of 20 mg/ml bovine serum albumin (BSA), the solution was incubated at room temperature for another 1 h. Beads were washed in PBS containing 1 mg/ml BSA and stored at 4°C in 500 μl of PBS containing 0.2 mg ml/BSA. To determine the coupling efficiency, the protein concentration of the starting solution and of the supernatant after coupling was determined. Integrity of coated fusion protein was checked using Western blot analysis. Beads coated with GST, GST-Inv397, or GST-FnBPA-Du-D4 were referred to as GST-beads, Invasin-beads, or FnBPA-beads, respectively. For infection assays, the volume giving rise to a beads-to-cell ratio of 100:1 was added to the cells.

Microinjection of Proteins

For microinjection experiments cells were seeded onto glass coverslips 1 d before the experiment. Microinjection was performed by using a transjector 5246 (Eppendorf, Hamburg, Germany) and a Compic inject micromanipulator (Cell Biology Trading, Hamburg, Germany). Proteins were injected into the cytoplasm at 0.7–1 mg/ml. Injected cells were identified by coinjected rat IgG (0.5 mg/ml; Dianova, Hamburg, Germany) after staining with fluorescein isothiocyanate (FITC)-labeled goat anti-rat IgG (Dianova).

Ligand Overlay Assay

The ligand overlay assay was performed as described previously (Hussain *et al*., 2001).

Immunofluorescence

Inside/outside staining for the discrimination between intracellular and extracellularly attached beads or bacteria was performed as described previously (Wiedemann *et al*., 2001). Briefly, cells were fixed with PBS containing

4% paraformaldehyde for 5 min and then incubated with antibodies directed either against *S. aureus*, invasin or GST in the appropriate dilutions (see above). Subsequently, cells were washed three times followed by incubation with Alexa Fluor 568-labeled goat anti-rabbit IgG (diluted 1:200) (Invitrogen). After cell permeabilization with ice-cold acetone for 5 min, coverslips were incubated with antibodies directed either against *S. aureus*, invasin, or GST followed by incubation with Alexa Fluor 488-labeled goat anti-rabbit IgG (1:200) (Invitrogen). Thereby, intracellular bacteria are in green and extracellular bacteria are in yellow/orange due to overlay of two fluorescence dyes. For evaluating the amount of invaded beads or bacteria, the number of invaded and total cell-associated beads/bacteria was counted microscopically.

Images from fixed samples were acquired with a Leica DMRBE microscope equipped with a Spot camera (Visitron Systems, Puchheim, Germany) controlled by MetaMorph (Molecular Devices, Sunnyvale, CA), except Figure 5B, which was imaged with an UltraView LCI spinning disk confocal system (see below). Live cell experiments and z-staples for the three-dimensional (3D)-model in Figure 5B were performed with an UltraView LCI spinning disk confocal system (PerkinElmer Life and Analytical Sciences, Rodgau-Jügesheim, Germany) fitted on a Nikon TE300 microscope equipped with a temperature- and CO_2-controllable environment chamber. Images were taken with the black/white ORCA ER camera (Hamamatsu, Herrsching, Germany).

Software and Calculations

Processing of the z-staples for 3D-reconstruction was performed with Volocity (Improvision, Tübingen, Germany). For tracking of beads and evaluation of velocity and distance to origin values, MetaMorph software (Molecular Devices) was used. Briefly, an overlay of the threshold image depicting the beads (orange), and the phase contrast was generated. The distance of beads between single frames was determined using the software, and then mean speed was calculated. Distance to origin is the mean distance of all beads at the given time points. For evaluating the fluorescence intensity traces, Ultraview LCI software (PerkinElmer Life and Analytical Sciences) was used. A region of interest was defined around the bacteria, and gray level values were logged for each wavelength. Quicktime movies were generated with ImageJ (Rasband, 2006).

RESULTS

Kinetics of FnBPA-mediated Internalization of Staphylococci by Primary Human Endothelial Cells

Invasion of cells via *S. aureus* FnBPA requires an Fn bridge between FnBPA and the $\alpha5\beta1$ integrin (Sinha *et al*., 1999). In comparison, the surface protein invasin of enteropathogenic yersiniae directly binds to $\beta1$-integrins to trigger cell invasion (Dersch and Isberg, 1999; Isberg *et al*., 2000). To get a first idea about the dynamics of these two bacterial invasion processes, we used *S. aureus* DU 5883(pFnBA4), which expresses FnBPA (*FnBPA-S. aureus*; Greene *et al*., 1995), and *E. coli* HB101, which expresses invasin (*Invasin-E. coli*; Schulte *et al*., 1998), and we performed time courses of bacterial invasion into primary HUVECs.

As documented in Figure 1, A and B, the invasion rates of *FnBPA-S. aureus* and *Invasin-E. coli* into HUVECs differed markedly. After 10 min, >80% of cell attached *Invasin-E. coli* were internalized, whereas in the same time period only ~20% of *FnBPA-S. aureus* were taken up. Further internalization of *FnBPA-S. aureus* proceeded almost linearly, reaching ~80% at 120 min (Figure 1B). The internalization kinetics of *S. carnosus* TM300(pFNBA4), which heterologously expresses FnBPA (Sinha *et al*., 2000), was indistinguishable from that of *FnBPA-S. aureus* (our unpublished data).

To verify these results in a bacteria-free system, we tested invasion of 1-μm-diameter latex beads coated with the 31-kDa Du-D4 segment of *S. aureus* FnBPA (FnBPA-beads). The Du-D4 segment harbors most of the Fn-binding repeats of FnBPA (Massey *et al*., 2001), and we confirmed its Fn-binding activity by ligand overlay assay (our unpublished data; Hussain *et al*., 2001). Likewise, invasion of beads coated with the 42-kDa $\beta1$-integrin binding fragment of *Yersinia enterocolitica* invasin was tested (Invasin-beads; Wiedemann *et al*., 2001). As shown in Figure 1B, internalization kinetics of FnBPA-beads and Invasin-beads closely resembled that of *FnBPA-S. aureus* and *Invasin-E. coli*, respectively. These data show that staphylococci expressing FnBPA spend in the mean ~45 min on the endothelial cell surface before being ingested. Because most *Invasin-E. coli* were internalized within 5–10 min, we conclude that the molecular mechanisms regulating invasin- and FnBPA/Fn-mediated invasion are different.

In our assay FnBPA on the surface of staphylococci or beads binds to serum Fn thus producing Fn-coated particles (Figure 1C; our unpublished data). We were interested to find out whether the Fn coat is necessary or sufficient for cell invasion and whether Fn aggregates and fibrils that are usually exposed on the surface of cultured endothelial cells also promote invasion. Because endogenous Fn production cannot be completely eliminated in HUVECs, we determined invasion of *FnBPA-S. aureus* pretreated with or without fetal calf serum (producing Fn-coated- and uncoated bacteria, respectively) into $Fn^{-/-}$ fibroblasts (Nyberg *et al*., 2004) As shown in Figure 1C, $Fn^{-/-}$ cells cultured in serum-free medium are devoid of cellular Fn. Fn-coated *FnBPA-S. aureus* was readily internalized by $Fn^{-/-}$ fibroblasts, but no internalization of uncoated bacteria was detected (Figure 1D). We next tested whether uncoated *FnBPA-S. aureus* was internalized by HUVECs that expose Fn matrix on the surface (Figure 1C). The HUVECs internalized uncoated *FnBPA-S. aureus* with comparable efficiency as the Fn-coated bacteria (Figure 1D). These experiments demonstrate that both serum Fn and cellular Fn are competent to promote FnBPA-mediated cellular invasion.

S. aureus FnBPA Induces Formation of Fibrillar Adhesion-like Structures on the Surface of Endothelial Cells

Clustering of integrins by extracellular matrix proteins leads to the formation of distinct adhesion structures (Zamir and Geiger, 2001), and we therefore asked what type of adhesions are induced by FnBPA/Fn. First, we devised an assay that can distinguish between focal adhesions/focal complexes and fibrillar adhesions (also termed ECM contacts) in HUVECs. For this, a GFP-fusion of the focal- and fibrillar adhesion protein tensin (GFP-tensin) was expressed in HUVECs, and the latter were concomitantly stained for the focal adhesion proteins vinculin, paxillin, or phosphorylated focal adhesion kinase (pFAK). Streak-like enrichments of vinculin in the cell periphery that colocalized with GFP-tensin were identified as focal adhesions (Figure 2A). These structures also contained paxillin and pFAK (our unpublished data). In comparison, streaky and beaded accumulations of GFP-tensin that mostly localized toward the cell center represent fibrillar adhesions (Figure 2A). As in other cell types, the fibrillar adhesions of HUVECs contained no paxillin or pFAK but colocalized with $\alpha5$ integrin subunits (our unpublished data). Consistent with its proposed translocation out of focal adhesions, GFP-tensin often seemed to form a centripetal extension of vinculin streaks (Figure 2A, overlay 2).

Next, we evaluated which adhesion proteins were recruited by FnBPA- and Invasin-beads. As demonstrated in Figure 2B, GFP-tensin accumulated in cup-like structures around both types of beads, whereas vinculin was only recruited by the Invasin-beads. Quantitative analyses verified that vinculin, paxillin, and pFAK only rarely were corecruited with GFP-tensin by the FnBPA-beads. In contrast, in the majority of cases these adhesion proteins were corecruited with GFP-tensin by the Invasin-beads (Figure 2C). For example, 17% of the GFP-tensin cups induced by FnBPA-beads compared with 97% induced by the Invasin-beads recruited vinculin (Figure 2C).

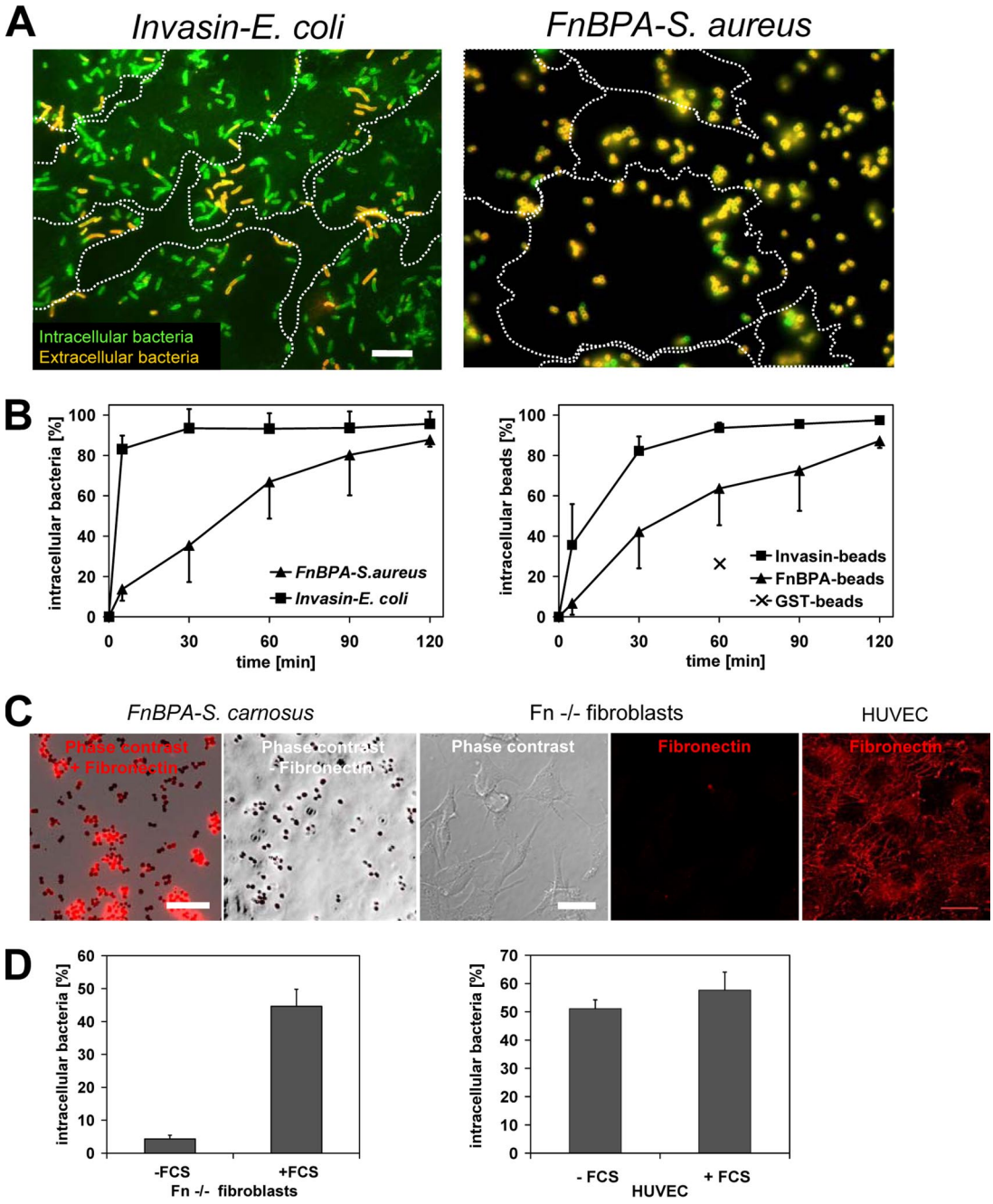

Figure 1. Kinetics and fibronectin dependence of FnBPA-mediated invasion of staphylococci by HUVECs. (A) Fluorescence images of HUVECs infected with *Invasin-E. coli* or *FnBPA-S. aureus*. Cells were infected for 10 min by using a bacteria-to-cell ratio of 30:1 and immunostained to distinguish extra- and intracellular bacteria (see *Materials and Methods*). Intracellular bacteria are green, and extracellular bacteria are orange. Dotted lines outline cell margins. Most *Invasin-E. coli* are intracellular, whereas most *FnBPA-S. aureus* are extracellular. Bar, 10 μm. (B) Uptake kinetics of *FnBPA-S. aureus* and *Invasin-E. coli* (left) or Invasin-beads and FnBPA-beads (right). HUVECs were infected with a beads/bacteria-to-cell ratio of 50–100:1. At indicated time points, cells were fixed, and extracellular bacteria/beads were immunostained. Percentage of invaded beads/bacteria was determined microscopically by subtracting extracellular from total number of cell-associated beads/bacteria. The internalization rate of GST-beads at 60 min was included (x in right panel). Each data point represents mean ± SD of three different experiments with at least 100 cells (~5000–10,000 beads/bacteria) evaluated per experiment. (C) Fibronectin staining of *FnBPA-S. carnosus*, $FN^{-/-}$ fibroblasts and HUVECs. *FnBPA-S. carnosus* was transferred or not to standard HUVECs growth medium containing 2% fetal calf serum. $Fn^{-/-}$ fibroblasts and HUVECs were grown in serum-free- and standard medium, respectively. Bacteria or cells were subjected to immunofluorescence staining for fibronectin and evaluated by microscopy. Bars, 10 μm. (D) Internalization rates of Fn-coated and uncoated *FnBPA-S. aureus* into fibronectin-knockout ($Fn^{-/-}$) fibroblasts (left) or HUVECs (right). *FnBPA-S. aureus* were preincubated in medium without or with fetal calf serum (±FCS) producing uncoated- or Fn-coated (see C) bacteria, respectively. $Fn^{-/-}$ fibroblasts were grown in serum-free medium, and HUVECs pregrown in standard medium were washed and kept in serum-free standard medium for 1 h before addition of a bacteria-to-cell ratio of 100:1 for 1 h. The percentage of intracellular bacteria was determined microscopically by subtracting extracellular from total number of cell-associated bacteria. Each bar represents mean ± SD of three different experiments with at least 100 cells counted per experiment.

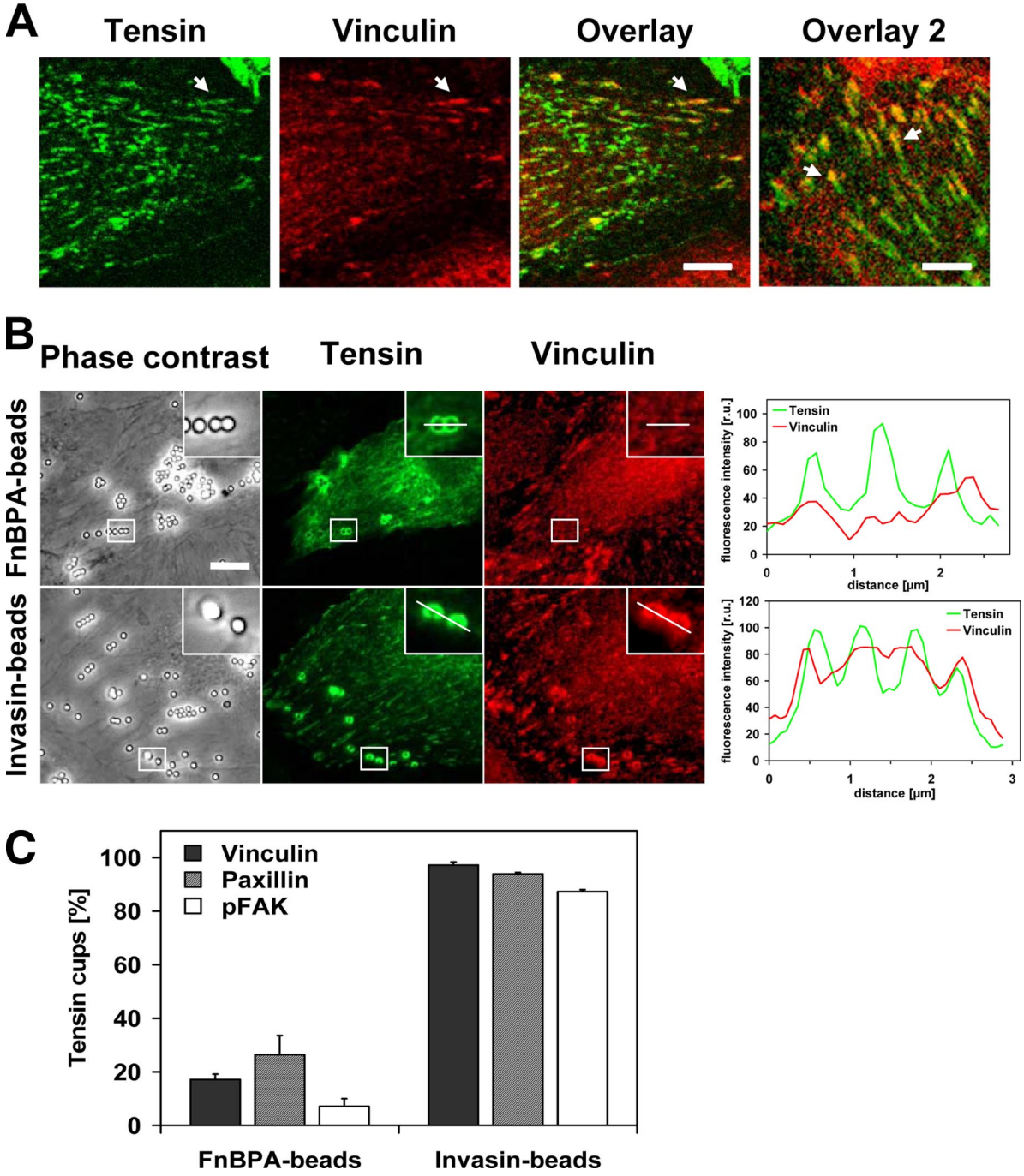

Figure 2. FnBPA induces formation of fibrillar adhesion-like bacterial attachment sites on HUVECs. (A) Confocal fluorescence images of HUVECs showing tensin and vinculin localization. HUVECs were transfected with GFP-tensin and immunostained with anti-vinculin antibody. Arrows in the overlay indicate vinculin and tensin colocalization (orange) in peripheral focal adhesions. Arrows in overlay 2 indicate bipartite adhesions containing vinculin and tensin (orange) in the peripheral part and only tensin (green) in the central part. Bar, 6 μm in first overlay and 5.5 μm in overlay 2. (B) Recruitment of tensin and vinculin by FnBPA-beads and Invasin-beads in HUVECs. GFP-tensin transfected HUVECs were infected with FnBPA-beads or Invasin-beads at a beads-to-cell ratio of 50–100:1 for 1 h. Cells were immunostained for vinculin. Bar, 10 μm. Intensity traces of GFP-tensin (green) and vinculin (red) at attachment sites of FnBPA-beads or Invasin-beads. Fluorescence intensity was measured along the white line shown in the insets and plotted against the distance. (C) Corecruitment of focal adhesion proteins to GFP-tensin–positive FnBPA-beads and -Invasin-beads. GFP-tensin transfected HUVECs were infected with FnBPA-beads or Invasin-beads at a beads-to-cell ratio of 50–100:1 for 1 h. Cells were then immunostained for vinculin, paxillin, or pFAK. The number of GFP-tensin–positive beads that were also positive for the respective adhesion protein was determined microscopically. Each bar represents mean ± SD of three different experiments with at least 100 GFP-tensin cups evaluated cells per experiment.

These data indicate that the adhesion structures produced by FnBPA-beads on the surface of HUVECs most closely resemble fibrillar adhesions. *FnBPA-S. aureus* and *-S. carnosus* had the same effect as FnBPA-beads (our unpublished

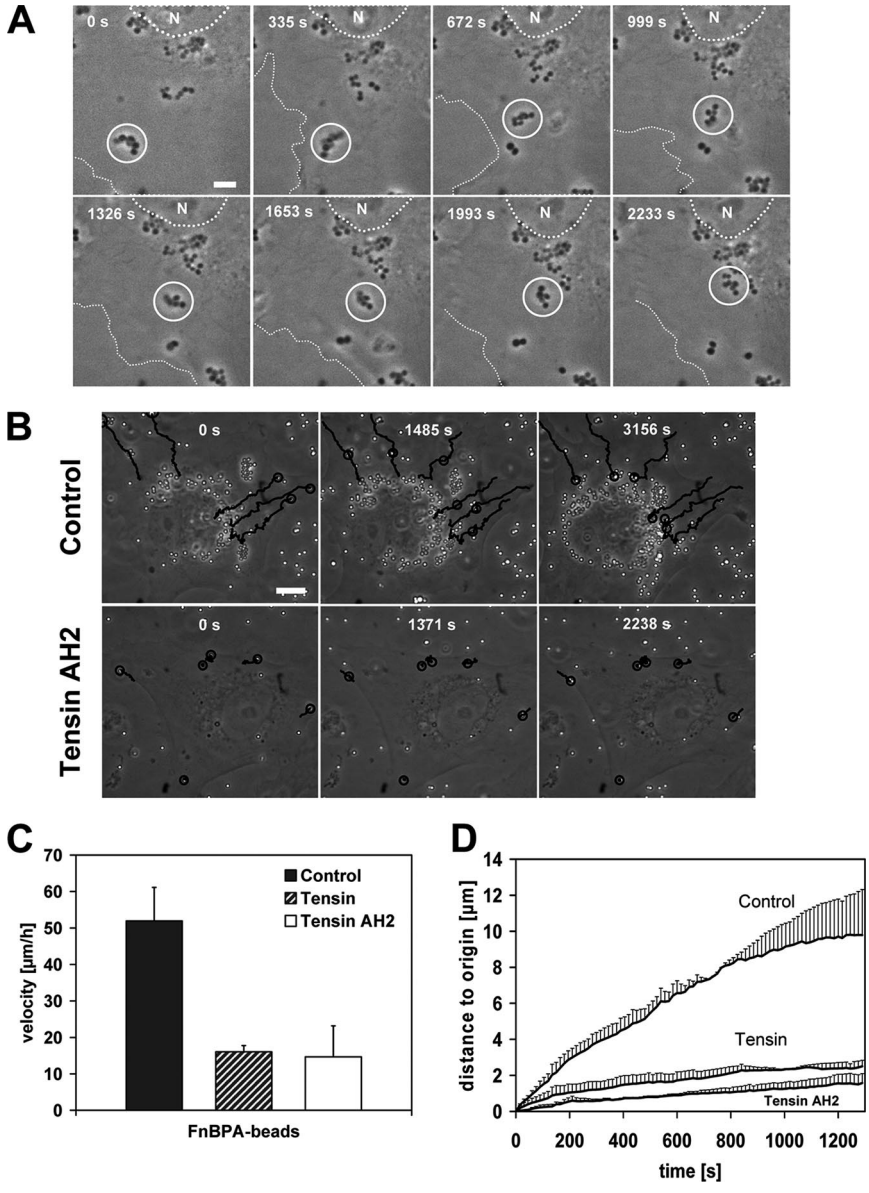

Figure 3. FnBPA-mediated bacterial movements are controlled by tensin. (A) Movement of an *FnBPA-S. carnosus* cluster on HUVECs. Cells were infected with *FnBPA-S. carnosus* and subjected to live cell imaging (details in *Materials and Methods*). The depicted phase contrast images were taken from a movie at the indicated time points (Supplemental Movie 1). Circle highlights the position of the moving bacterial cluster. Dotted line outlines the nucleus (N) and broken line the cell margin. Bar, 5 μm. (B) Effect of tensin AH2 overexpression on FnBPA-bead movements. HUVECs expressing GFP (control) or GFP-tensin AH2 were infected with FnBPA-beads and subjected to live cell imaging. The depicted phase-contrast images were taken from the movies at the indicated time points (Supplemental Movies 2 and 3). Tracks of selected FnBPA-beads are indicated by lines. Circle points out the actual position of the beads on their track. Bar, 10 μm. (C) Velocity of FnBPA-beads in HUVECs overexpressing tensin or tensin AH2. GFP-, GFP-tensin-, or GFP-tensin AH2-expressing HUVECs were infected with FnBPA-beads and subjected to live cell imaging. Bead movements were tracked and velocities were calculated. Each bar represents mean ± SD from nine (GFP-tensin), 21 (GFP-tensin AH2), or 19 (GFP/control) values obtained in two to four different experiments. (D) Same experiment as in C, but the distances that beads covered relative to the starting point (0 s) are depicted.

data). In contrast, the attachment sites generated by Invasin-beads and *Invasin-E. coli* resemble classical focal adhesions (Figure 2, B and C).

FnBPA-mediated Bacterial Movements on the Surface of Endothelial Cells Are Controlled by Tensin

It has been proposed that fibrillar adhesions develop from focal adhesions by actomyosin-driven centripetal translocation (Pankov *et al.*, 2000; Zamir *et al.*, 2000). To investigate whether the fibrillar adhesion-like attachments sites generated by the staphylococci might mediate bacterial translocation, we used time-lapse videomicroscopy. These recordings in fact documented centripetal movements of *FnBPA-S. carnosus* clusters and FnBPA-beads, which usually started at the cell edges and proceeded in the direction of the cell center (single frames of representative Movies 1 and 2 are shown in Figure 3, A and B; see Supplemental Movies 1 and 2). Essentially all (95%) of the bacteria at the cell periphery moved centripetally. Stationary particles likely represent internalized bacteria that have already reached their final lysosomal localization. The velocity of the beads or bacteria moving on the cell surface was ~50 μm/h and therefore was somewhat higher than the velocity of 18 μm/h reported for fibrillar adhesions at the cell bottom (Zamir *et al.*, 2000). *Invasin-E. coli* also translocated in HUVECs, which reflected intracellular transport of bacteria-containing phagosomes (our unpublished data).

We next wanted to find out whether FnBPA-bead movements are indeed governed by the fibrillar adhesions and their central component tensin. Overexpression of both wild-type tensin and its dominant-negative AH2 domain has been shown to modulate the function of endogenous tensin or to disrupt fibrillar adhesions in cells (Pankov *et al.*, 2000; Chen *et al.*, 2002; Chen and Lo, 2003). To quantify FnBPA-bead movements, we measured bead velocity and the distance the beads covered within a certain time period relative to origin (distance to origin). As documented in Figure 3C, bead velocity was diminished by ~70% in cells overexpressing GFP-tensin or GFP-tensin AH2 compared

with control cells expressing GFP. Moreover, in the GFP-tensin– or GFP-tensin AH2-overexpressing cells, the distance to origin covered by the FnBPA-beads was reduced drastically by 80–90% (Figure 3D). In these cells, bead movements were mainly confined to the cell margins (Figure 3B and Supplemental Movie 3).

Together, these experiments indicate that the fibrillar adhesion protein tensin controls centripetal movements of FnBPA-exposing staphylococci and -beads on the endothelial cell surface.

FnBPA-stimulated Integrin Signaling Induces Formation of Multiple Actin Cups

It has been reported that FnBPA-mediated cellular invasion of staphylococci is associated with formation of actin-rich phagocytic cups (Agerer *et al*., 2005). We confirmed this by rhodamine phalloidin staining of *FnBPA-S. carnosus*-infected HUVECs and also verified by selective immunofluorescence staining that all bacteria encompassed by actin cups are localized extracellularly (our unpublished data).

For monitoring how actin cup formation is coordinated with bacterial movement, live cell imaging of GFP-actin–expressing cells infected with *FnBPA-S. carnosus* was used. It was revealed that GFP-actin repeatedly accumulated around clusters of staphylococci, whereas these were translocating on the cell surface (single frames of a representative movie are depicted in Figure 4A; see Supplemental Movie 4). A higher spatiotemporal resolution showed that during one accumulation event GFP-actin in fact advances in a wave-like manner from one end of the staphylococcal chain to the other. By this, cup formation around individual bacteria in the chain was accomplished (Figure 4B, top; see Supplemental Movie 5). In some cases, it even seemed as if vigorous actin bursts were capable of separating bacterial clusters (Figure 4B, bottom). In experiments using single FnBPA-beads, it was found that these beads triggered up to 10 separate GFP-actin cups, whereas Invasin-beads never produced more than two actin cups (Figure 4C). A fluorescence intensity trace of GFP-actin repeatedly accumulating around a FnBPA-bead doublet is depicted in Figure 4D. From this and similar experiments, it was determined that the duration of the actin accumulation at single cups is very constant (80 ± 33 s; mean $\pm$ SD; $n = 44$), whereas the intermittent periods vary widely (range 21–1200 s).

To show the relevance of the described actin reorganizations for FnBPA-mediated invasion, we tested the effect of Rho GTPase- and N-WASp inhibitors. Rho GTP-binding proteins are universal regulators of actin and for integrin-triggered phagocytic cup formation they have been shown to engage N-WASp and Arp2/3 complex (May and Machesky, 2001; Wiedemann *et al*., 2001). Microinjection of the Rho-inhibitor C3-transferase, dominant inhibitory N17Rac, or N17Cdc42, or treatment with the N-WASp inhibitor wiskostatin all reduced internalization of *FnBPA-S. aureus* by 50–60% (Figure 4E). This indicates that the actin cups assembled by cooperation of different RhoGTPases and N-WASp crucially control FnBPA-mediated invasion. Consistent with this, GFP-fusions of Rac, Cdc42, and N-WASp translocated together with mRFP-actin to phagocytic cups (our unpublished data).

FnBPA-stimulated Actin Comet Tails Propel Bacteria on the Cell Surface

While analyzing phase-contrast movies of infected cells, we regularly observed motions of FnBPA-expressing staphylococci that seemed undirected and were much faster than the centripetal movements described above. Such motions were also seen with FnBPA-beads; they occurred about once every 10 min per recorded cell (mean of 13 single cell recordings) and displayed a velocity of 400-1000 μm/h (single frames of a representative movie are depicted in Figure 5A; see corresponding Supplemental Movie 6A). An explanation for these fast bacterial movements was obtained in recordings of GFP-actin–expressing HUVECs. These movies visualized GFP-actin comet tails that propelled bacteria forward with a velocity of up to 1000 μm/h (14 events analyzed; see Supplemental Movie 6B, which is the parallel recording of Supplemental Movie 6A). Rhodamine-phalloidin staining of infected HUVECs confirmed the existence of bacterial comet tails consisting of endogenous actin (our unpublished data). Quantification revealed that $27 \pm 15\%$ of all cell-associated bacteria showed actin accumulations (mean $\pm$ SD of 28 recordings), and of these roughly 13% were comet tails (mean of 7 recordings). Comet tails could constitute one of several cycles of actin accumulation at FnBPA-expressing bacteria or beads, in a way that an actin cup was followed by a comet tail and again by an actin cup. Comet tails could form spontaneously, but they could also directly form from an actin cup. Thus, actin cups and comet tails are likely different expressions of the same phenomenon, with the comet tails being polarized, thereby causing propulsion of bacteria or beads. Because actin comet tails have so far been described mainly on intracellular bacteria, we tested whether the tails we observed were induced by extra- or intracellular staphylococci (Stevens *et al*., 2006). Selective extracellular immunofluorescence staining of staphylococci and 3D reconstruction of a comet tail documents that although the bacterial cell is largely engulfed by GFP-actin, its top still reaches into the extracellular space (Figure 5B). These experiments strongly support the idea that actin comet tails are produced by extracellular staphylococci.

Many pathogen-triggered actin comet tails are generated by activation of N-WASp that stimulates the actin nucleation activity of Arp2/3 complex (Stevens *et al*., 2006). We therefore visualized staphylococcal comet tails in cells coexpressing mRFP-actin and GFP-N-WASp or mRFP-actin and GFP-Arp3, the latter being a subunit of Arp2/3 complex (Welch *et al*., 1997). As depicted exemplary in Figure 5C, GFP-N-WASp was enriched in cup-like structures underneath bacteria producing an mRFP-actin comet tail. In comparison, GFP-Arp3 colocalized with mRFP-actin in the comet tail (Supplemental Movie 7). This suggests that N-WASp is recruited to the bacterial attachment site and assembles actin cups and comet tails via Arp2/3 complex. Consistent with this notion, no comet tails could be observed in cells treated with the N-WASp inhibitor wiskostatin.

Dynamic Interplay of Tensin, Actin, and Rab5 in FnBPA-stimulated Endothelial Cell Activation and Phagocytosis

Our data suggest that FnBPA induces an interplay of tensin and actin in endothelial cell phagocytic cups that eventually leads to bacterial invasion. To visualize the spatiotemporal regulation of this interplay, live cell imaging of *FnBPA-S. aureus*–infected HUVECs coexpressing mRFP-actin and GFP-tensin was performed. As documented in Figure 6A (single frames of representative Movie 8; see Supplemental Materials), mRFP-actin and GFP-tensin dynamically redistributed around bacterial clusters translocating on the cell surface. When mRFP-actin accumulated at one or more cells of the bacterial tetrad, there was a discrete to extensive colocalization with GFP-tensin. Intensity traces demonstrate that during the phases of mRFP-actin accumulation at phagocytic cups the level of GFP-tensin also increased lo-

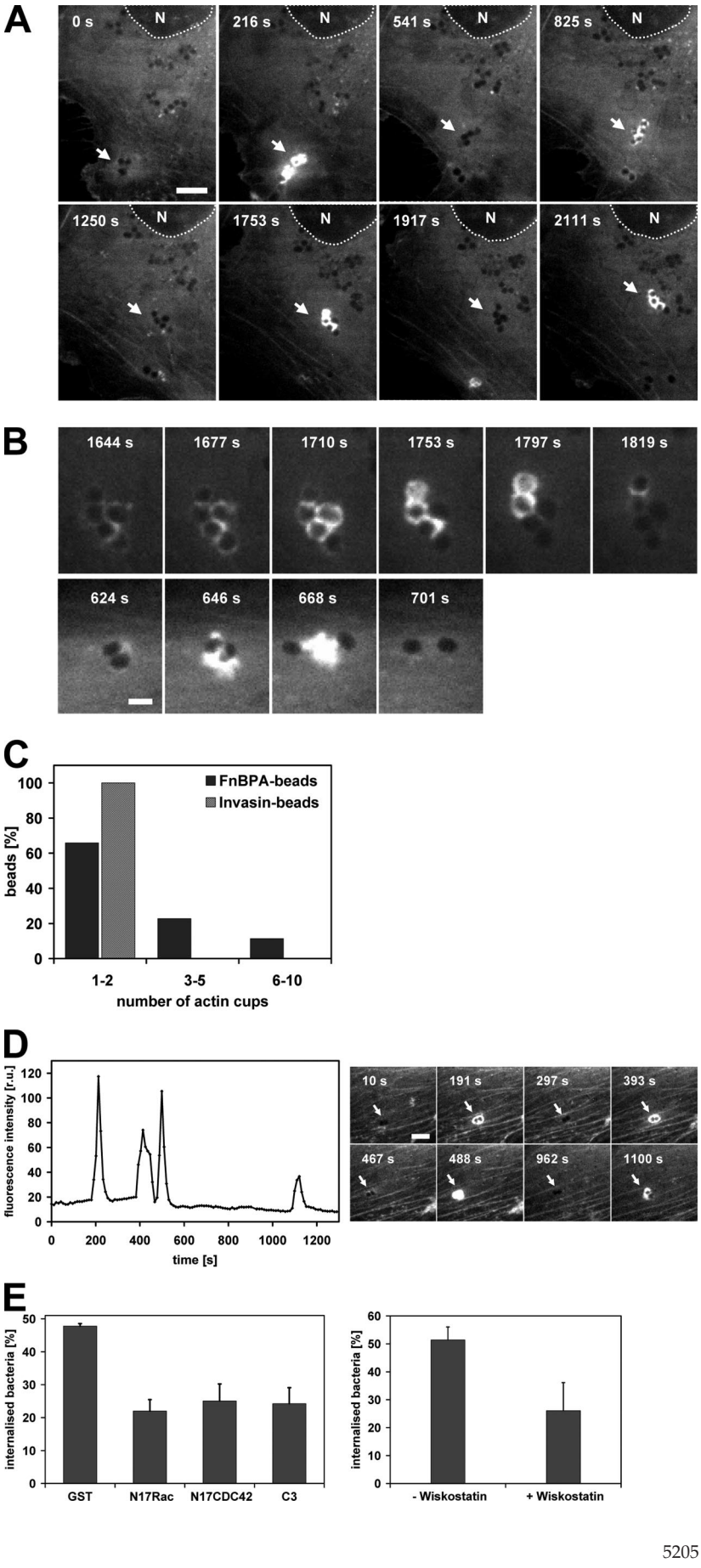

Figure 4. Periodic formation of actin cups induced by FnBPA-coated particles on HUVECs. (A) Periodic actin recruitments by an *FnBPA-S. carnosus* cluster moving on HUVECs. GFP-actin expressing HUVECs were infected with *FnBPA-S. carnosus* and subjected to live cell imaging (same experiment as shown in Figure 3A and Supplemental Movie 1 but showing the GFP fluorescence channel). The depicted fluorescence images were taken from Supplemental Movie 4 at the indicated time points. Arrows point to the position of the moving bacterial cluster. Dotted line outlines the nucleus (N). Bar, 5 μm. (B) Top, higher spatiotemporal resolution of GFP-actin dynamics at the moving bacterial cluster of A (Supplemental Movie 5). Bottom, separation of a bacterial doublet into single bacteria by an actin burst. (C) Number of consecutive actin cups induced by single FnBPA-beads or Invasin-beads. GFP-actin transfected HUVECs were infected with FnBPA-beads or Invasin-beads. The number of separate actin cups induced by individual moving beads was determined. For FnBPA-beads, 44 tracks from seven movies and for Invasin-beads 61 tracks from seven movies were evaluated. The length of the recording times for individual tracks varied (up to 4200 s), but total observation time was essentially the same for the FnBPA- and Invasin-beads. (D) Intensity trace of GFP-actin at moving FnBPA-beads. GFP-actin recruitment by a moving bead doublet was recorded, and fluorescence intensity of GFP-actin in a defined area around the beads was plotted as a function of time. The depicted fluorescence images were taken from the movie at the indicated time points. Arrows point to the position of the doublet. Bar, 2.5 μm. (E) Effect of Rho GTPase- and N-WASp inhibitors on FnBPA-mediated uptake. Left, HUVECs were microinjected with GST alone or with GST-fusions of N17Rac, N17CDC42, or C3-transferase and incubated for 45 min. Cells were infected with *FnBPA-S. aureus* at a bacteria-to-cell ratio of 100:1 for 1 h. The percentage of internalized bacteria was determined as described in the legend to Figure 1B. Each bar represents mean ± SD of three different experiments with at least 100 cells counted per experiment. Right, N-WASp inhibitor wiskostatin was added to HUVECs 30 min before infection with *FnBPA-S. aureus*, and the internalization assay was performed as described above.

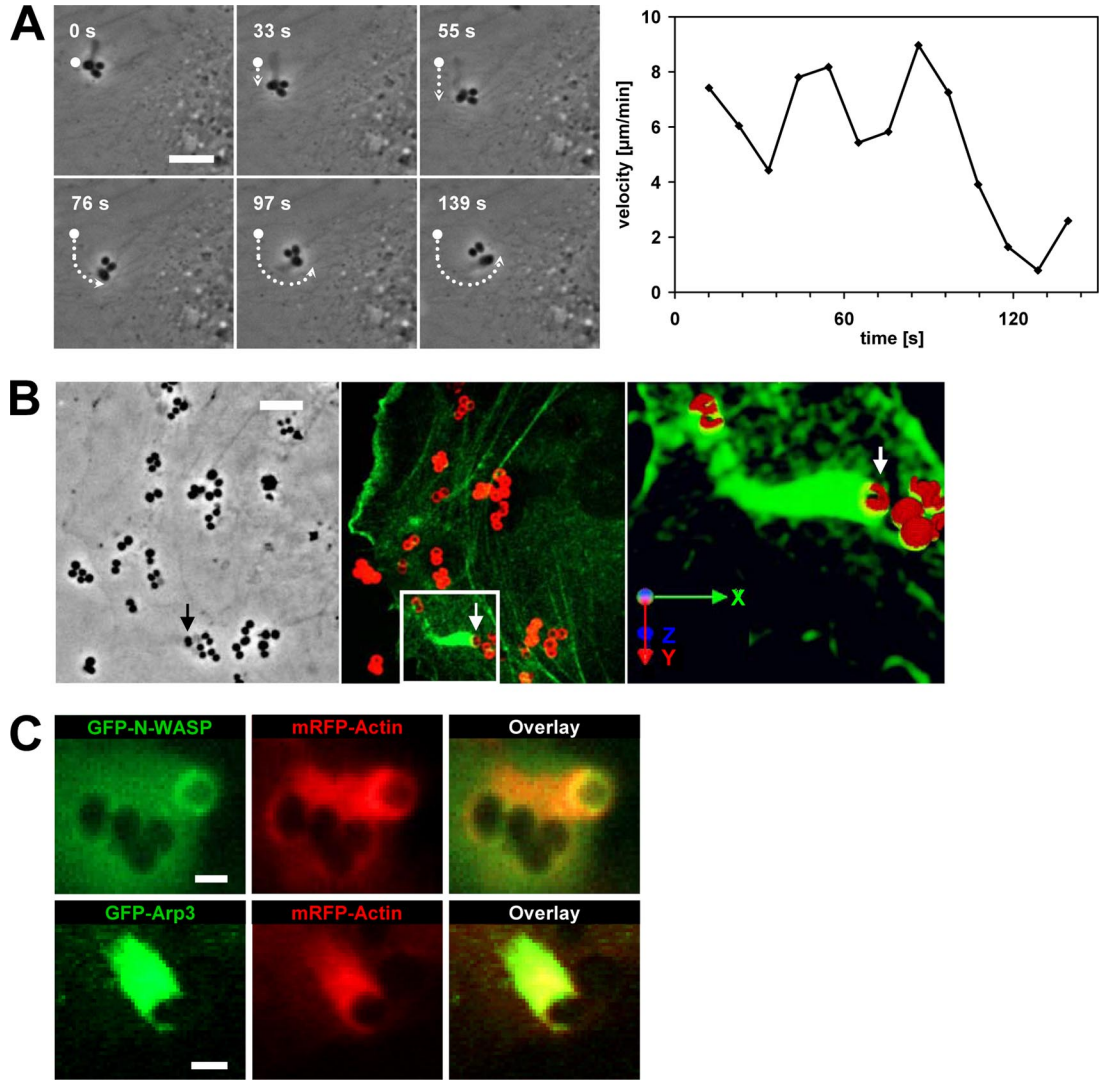

Figure 5. FnBPA triggers actin comet tails that propel the bacteria on the endothelial cell surface. (A) Fast motions of *FnBPA-S. carnosus* on HUVECs. HUVECs infected with *FnBPA-S. carnosus* were subjected to live cell imaging. The depicted phase contrast images were taken from Supplemental Movie 6A at the indicated time points. Dot, dotted line, and arrow mark the starting position, covered distance, and current position, respectively, of a single bacterium in the cluster. Bar, 5 μm. Right, velocity of the marked bacterium at indicated time points. (B) GFP-actin-transfected HUVECs were infected with *FnBPA-S. aureus* for 1 h. Cells were fixed and extracellular staphylococci were stained with red fluorescing secondary antibody (see *Materials and Methods*). Left, phase contrast reference image of a bacterial doublet (arrow), which is associated with an actin tail as shown in the fluorescence image (middle; arrow). From the boxed area, z-staples were recorded and assembled to a 3D-image (right) that shows that the bacterial doublet (arrow) is almost completely engulfed by GFP-actin, but its top still reaches into the extracellular space. Axes depict the spatial orientation of the 3D model. Bar, 5 μm. (C) HUVECs coexpressing GFP-N-WASp and mRFP-actin or GFP-Arp3 and mRFP-actin were infected with *FnBPA-S. carnosus*, and comet tails were recorded by live cell imaging. GFP-N-WASp forms a cup underneath the bacterium, whereas mRFP-actin and GFP-Arp3 colocalize in the comet tail (Supplemental Movie 7). Bar, 1 μm.

cally at the bacteria (Figure 6A). These data are consistent with the idea that tensin regulates FnBPA-triggered actin cup formation. To further test this idea, we quantified the number of actin cups produced by *FnBPA-S. carnosus* in cells overexpressing GFP or dominant-negative GFP-tensin AH2. The percentage of actin cups produced by cell-attached bacteria was reduced by ~60% in the tensin AH2-expressing cells compared with controls (Figure 6B). Because an inhibition of actin cup formation should result in diminished internalization, we also determined the effect of GFP-tensin AH2 overexpression on phagocytosis of *FnBPA-S. carnosus*. As hypothesized, bacterial internalization was inhibited by ~70% in the tensin AH2-expressing cells (Figure 6C). Overexpression of GFP-tensin or GFP-tensin AH2 did not affect adhesion rates of bacteria or beads to cells (our unpublished data). We therefore conclude that tensin crucially controls FnBPA-mediated actin reorganization and phagocytosis of staphylococci in endothelial cells.

The repeated formation of actin cups induced by the FnBPA-expressing staphylococci may reflect unsuccessful attempts of phagocytosis. We reasoned that another clear indication for initiation but not completion of phagocytosis would be repeated early phagosome formation. We therefore imaged phagocytosing HUVECs coexpressing mRFP-actin and the early endosome marker GFP-Rab5. Rab5 is among the first components of nascent phagosomes (Miaczynska *et al*., 2004; Jordens *et al*., 2005). These recordings revealed that like mRFP-actin, GFP-Rab5 was repeatedly recruited by translocating bac-

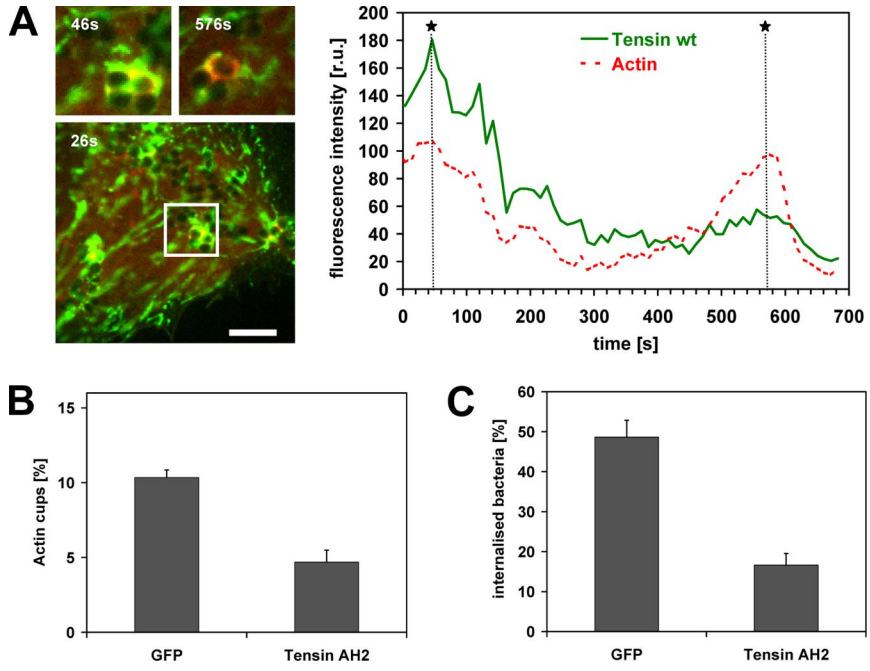

Figure 6. Dynamics of actin and tensin colocalization at phagocytic cups produced by *FnBPA-S. carnosus*. (A) Dynamic colocalization of actin and tensin at sites of *FnBPA-S. carnosus* attachment. HUVECs coexpressing GFP-tensin and mRFP-actin were infected with *FnBPA-S. carnosus* and subjected to live cell imaging. Because GFP-tensin overexpression strongly affects motility of FnBPA-staphylococci (see Figure 3D), we chose a cell with limited GFP-tensin expression and clearly motile cell surface bacteria as determined by probatory imaging. The depicted fluorescence images were taken from Supplemental Movie 8 at the indicated time points. The boxed area in the large fluorescence image contains a bacterial tetrad at which GFP-tensin and mRFP-actin colocalize (evident by yellow areas). This area is shown enlarged at later time points in the two small images on top. Bar, 5 μm. A fluorescence intensity trace of actin and tensin is shown in the right chart. Fluorescence intensities of mRFP-actin and GFP-tensin in a defined area around the bacterial tetrad were plotted as a function of time. Asterisks and dotted lines mark the time points at which the small enlarged fluorescence images were taken. (B) Tensin controls FnBPA-triggered actin cup formation. HUVECs expressing GFP or GFP-tensin AH2 were infected with *FnBPA-S. aureus* for 1 h. Actin phagocytic cups were visualized by rhodamine phalloidin staining and quantified. Each value represents mean ± SD of a representative experiment in which 100 cells were analyzed. (C) Tensin controls FnBPA-mediated internalization. HUVECs expressing GFP or GFP-tensin AH2 were infected with *FnBPA-S. aureus* for 1 h, and bacterial internalization was evaluated as described in the legend to Figure 1B. Each value represents mean ± SD of three different experiments with at least 33 cells analyzed per experiment.

terial clusters (single frames of exemplary Movie 9 are depicted in Figure 7A; see Supplemental Materials). The respective fluorescence intensity traces revealed that mRFP-actin and GFP-Rab5 localization at the staphylococci was mutually exclusive

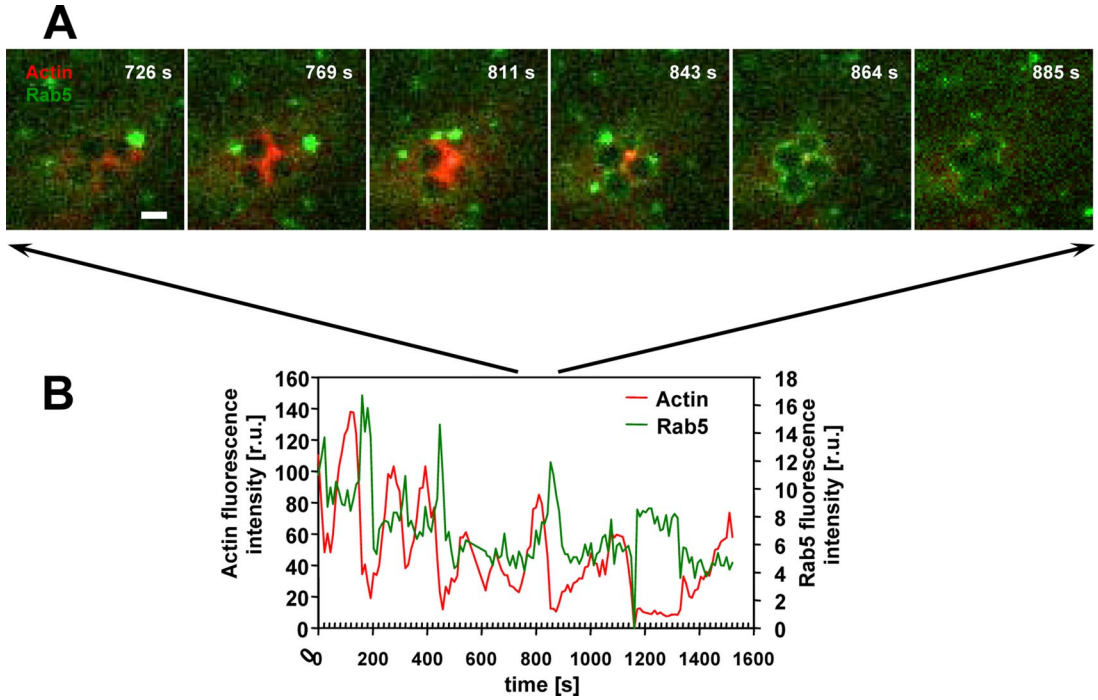

Figure 7. Periodic and alternating accumulation of actin and Rab5 at *FnBPA-S. carnosus*. HUVECs coexpressing GFP-Rab5 and mRFP-actin were infected with *FnBPA-S. carnosus* and subjected to live cell imaging (Supplemental Movie 9). (A) Fluorescence images were taken from Supplemental Movie 9 at the indicated time points. Bar, 1 μm. (B) Fluorescence intensities of mRFP-actin and GFP-Rab5 from a defined area around the bacterial tetrad shown in A were plotted as a function of time.

(Figure 7B). Interestingly, GFP-Rab5 accumulation regularly and reproducibly followed mRFP-actin accumulation after 40–50 s (Figure 7B; the time between the respective peak fluorescence intensities was measured). This temporal order goes well with the notion that actin drives internalization but is removed before phagosome formation (Scott *et al*., 2005). Yet, the repeated recruitments of GFP-Rab5 found here indicate that phagosome formation cannot be completed in the first attempts and again support the notion that FnBPA delays staphylococcal invasion. In successful internalization events, no actin accumulation followed after a strong Rab5 enrichment, and the bacteria-containing phagosome then rapidly moved toward the cell center (our unpublished data).

We conclude from these data that the cyclic actin dynamics stimulated by FnBPA/Fn in endothelial cells is carried on to Rab5 behavior. Together, these events suggest disturbance of actin and Rab5 coordination during invasion of FnBPA-expressing staphylococci in endothelial cells.

DISCUSSION

Although many bacterial adhesins induce efficient invasion of nonprofessional phagocytes, and FnBPA and FnBPB have been shown to be both required and sufficient for cellular invasion by *S. aureus* (Sinha *et al*., 2000), the findings presented here indicate that FnBPA-mediated invasion is particularly slow and inefficient. After binding to serum- or cellular Fn, FnBPA-expressing staphylococci generate fibrillar adhesion-like attachment sites on the surface of endothelial cells that promote bacterial movements and induce a cyclic recruitment of actin and Rab5. As a consequence, staphylococci remain on the cell surface for 45 min on average. In comparison, particles exposing *Yersinia* invasin produce attachment sites that are similar to focal adhesions and trigger bacterial internalization within a few minutes.

Seemingly in conflict with our results, it was reported that blockage of the focal adhesion regulatory protein FAK inhibited FnBPA-mediated phagocytosis in fibroblasts and human embryonic kidney cells (Agerer *et al*., 2005). However, given that fibrillar adhesions develop from focal adhesions, an indirect effect of focal adhesion disruption on fibrillar adhesion function is to be expected (Pankov *et al*., 2000; Zamir *et al*., 2000). Furthermore, fibrillar adhesion-like attachment sites may be more efficiently generated in primary endothelial cells, which belong to the most important physiological target cells of *S. aureus*.

According to current concepts recruitment of focal adhesion proteins to ligand-activated integrins is controlled by tractional forces exerted by the cells on the substratum and by tension within cells generated through actomyosin contraction (Katsumi *et al*., 2004). In our study using FnBPA- or invasin-coated beads attached to the cell surface the properties of the bacterial adhesins clearly determined focal adhesion protein recruitment. In this regard, the recent concept has to be considered that different ligand-activated conformational states of $\alpha5\beta1$-integrins exist that stimulate distinct intracellular signals (Mould *et al*., 2004; Clark *et al*., 2005). Presumably through direct and indirect integrin binding, respectively, invasin and FnBPA/Fn induce distinct modes of integrin activation, resulting in differential adhesion protein recruitment.

Rearward movements of Fn-coated beads on the cell surface have been analyzed previously (Choquet *et al*., 1997). However, in contrast to FnBPA-coated beads, Fn-coated beads are preferentially released when they approach the cell center (Nishizaka *et al*., 2000). Internalization, stimulation of actin remodeling, or regulation by tensin has not been described with Fn-coated beads. Instead, it was proposed that binding to FnBPA produces a conformational change in Fn or presents Fn molecules in way that alters their interaction with integrins (Schwarz-Linek *et al*., 2004). To find out whether and how Fn structure and function are altered by binding to bacterial adhesins is a major challenge for future studies.

The idea has been put forward that rearward flow of cortical actin filaments applies periodical force on Fn-ligated integrins and thereby pulls them toward the cell center (Giannone *et al*., 2004). One may speculate that dependent on the level of integrin coactivation, i.e., after Fn- or invasin binding, integrin-binding particles are either preferentially carried along with the actin flow or are efficiently internalized. According to our results, tensin may be involved in connecting FnBPA/Fn-ligated $\alpha5\beta1$ integrins and rearward flowing actin filaments. For this purpose, tensin contains a number of suitable domains such as a region binding to integrin β-subunits, a src homology 2 domain and multiple regions binding to actin (Chen and Lo, 2003; Lo, 2004). Together, these data indicate that tensin receives input from integrins to which Fn-binding staphylococci have attached, and it transmits these signals to the actin cytoskeleton that in turn regulate movements, phagocytic cup formation, and eventual invasion.

Interestingly, overexpression of both wild-type tensin and tensin AH2 inhibited motility of FnBPA-*S. aureus*. To investigate this further, we visualized fibrillary adhesions by using anti-$\alpha5$ integrin antibody in tensin- and tensin AH2-overexpressing cells. We confirmed that expression of tensin AH2 disrupted fibrillary adhesions (Pankov *et al*., 2000). We also found that overexpression of tensin increased the number of fibrillary adhesions in the endothelial cells (Supplemental Figure 1S). However, the fibrillary adhesions in the tensin-overexpressing cells seemed rigid and much less motile than controls. It seems therefore that artificially increasing the number of fibrillary adhesions disturbs their motility.

We showed that actin regulation during FnBPA-stimulated generation of phagocytic cups and comet tails is similar to that in other motile processes, i.e., involves Rho GTPases, N-WASp, and Arp2/3 complex. However, in contrast to intracellular bacteria such as *Listeria* and *Shigella*, the extracellular staphylococci trigger N-WASp and Arp2/3 complex activation across the plasma membrane via integrins. Although integrin outside-in signaling to actin apparently involves tensin, the incomplete blockage of actin cup formation by dominant-negative tensin AH2 suggests contribution of other signaling mechanisms.

To the most intriguing findings of our live cell-imaging experiments belongs the complexity of actin reorganization triggered by FnBPA-exposing bacteria or beads on the endothelial cell surface. This includes formation of 1) multiple sequential actin cups at moving bacteria, 2) actin waves advancing along bacterial chains, and 3) actin comet tails further accelerating the bacteria. Previously, it was reported that 1–4 h after infection of epithelial cells with *Listeria monocytogenes*, repeated cycles of actin assembly and disassembly were visible at the bacteria-containing phagosomes. This phenomenon called "actin flashing" clearly happened intracellularly but resembled formation of FnBPA-induced actin cups with regard to kinetics (cycles of ~80-s duration), morphology and involvement of Arp2/3 complex (Yam and Theriot, 2004). Together, this shows that a common actin polymerization machinery can be exploited by pathogens with distinct morphologies, attachment mechanisms, or cellular localizations to produce actin cups and comet tails.

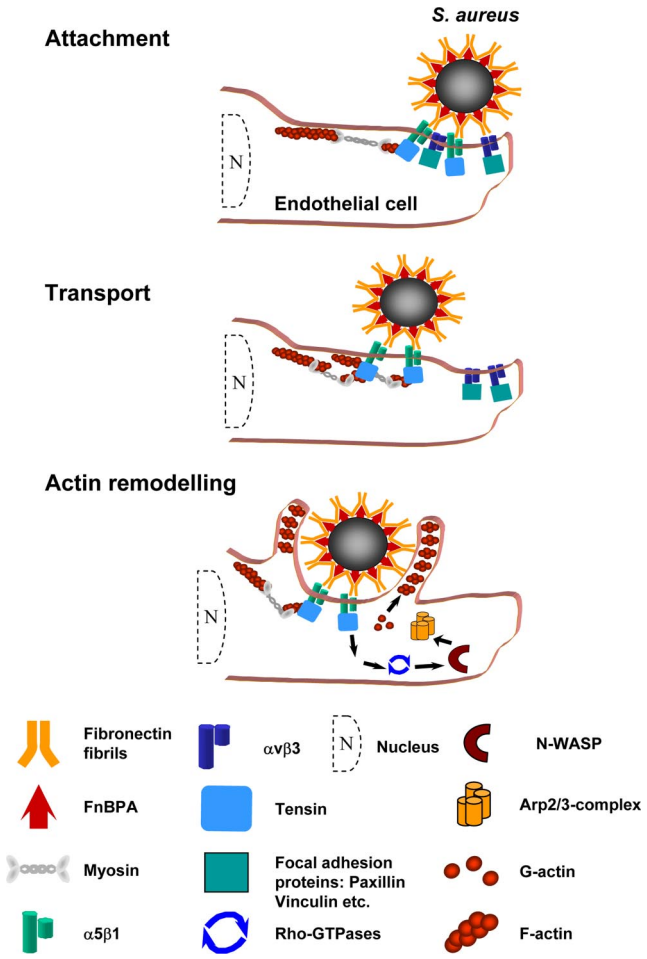

Figure 8. Dynamic processes during *S. aureus* attachment and invasion in endothelial cells. (A) Attachment of *S. aureus* to integrins at the periphery of an endothelial cell. (B) Transport of the staphylococci together with fibillar adhesion-like structures toward the cell center. (C) Tensin-mediated actin reorganization resulting in actin cup formation and eventual uptake. This model integrates results of our study and published properties and regulatory principles of fibrillar adhesions (Pankov *et al*., 2000; Zamir *et al*., 2001; Zamir and Geiger, 2001).

Finally, the repeated assembly of actin phagocytic cups and early phagosomes may be purposely induced by the staphylococci to delay phagocytosis. This may give the staphylococci enough time to produce critical amounts of cell damaging toxins. Consistent with this idea, it was reported that unless they exerted a high cellular toxicity before uptake, most *S. aureus* strains got efficiently eliminated in lysosomes of keratinocytes or endothelial cells (Krut *et al*., 2003; Schröder *et al*., 2006). Yet, for a host cell, the cyclic actin cup and phagosome formation may also somehow prepare the bacteria for eventual invasion. For example, proteases released from early phagosomes could digest and reprogram the FnBPA-bound Fn, enabling its uptake together with the bacteria (Sottile and Chandler, 2005).

In summary, the data presented here provide an example of the intricacies of *S. aureus*–host cell cross-talk and give new insight into both bacterial pathogenicity and Fn reorganization by the endothelium. A scheme of the proposed spatiotemporal processes during *S. aureus* invasion of endothelial cells is shown in Figure 8.

ACKNOWLEDGMENTS

We thank Muzaffar Hussain for help with the ligand overlay assay; Drs. Shin Lin, Silvia Lommel, Dorothy Schafer, and Craig Roy for providing GFP-fusion constructs; and Jürgen Heesemann for generous support. The expert technical assistance of Claudia Trasak and Sabrina Schubert is greatly appreciated. This work is part of the doctoral thesis of A.S. Work of our laboratories has been supported by Deutsche Forschungsgemeinschaft Grants SPP1130 and SFB 576 (to M.A. and R.F.) and in part by IZKF Münster Grant Si2/039/06 (to Bhanu Sinha).

REFERENCES

Agerer, F., Lux, S., Michel, A., Rohde, M., Ohlsen, K., and Hauck, C. R. (2005). Cellular invasion by *Staphylococcus aureus* reveals a functional link between focal adhesion kinase and cortactin in integrin-mediated internalisation. J. Cell Sci. *118*, 2189–2200.

Agerer, F., Michel, A., Ohlsen, K., and Hauck, C. R. (2003). Integrin-mediated invasion of *Staphylococcus aureus* into human cells requires Src family protein-tyrosine kinases. J. Biol. Chem. *278*, 42524–42531.

Brakebusch, C., and Fässler, R. (2003). The integrin-actin connection, an eternal love affair. EMBO J. *22*, 2324–2333.

Chen, H., Duncan, I. C., Bozorgchami, H., and Lo, S. H. (2002). Tensin1 and a previously undocumented family member, tensin2, positively regulate cell migration. Proc. Natl. Acad. Sci. USA *99*, 733–738.

Chen, H., and Lo, S. H. (2003). Regulation of tensin-promoted cell migration by its focal adhesion binding and Src homology domain 2. Biochem. J. *370*, 1039–1045.

Choquet, D., Felsenfeld, D. P., and Sheetz, M. P. (1997). Extracellular matrix rigidity causes strengthening of integrin-cytoskeleton linkages. Cell *88*, 39–48.

Chuang, J. Z., Lin, D. C., and Lin, S. (1995). Molecular cloning, expression, and mapping of the high affinity actin-capping domain of chicken cardiac tensin. J. Cell Biol. *128*, 1095–1109.

Clark, K., Pankov, R., Travis, M. A., Askari, J. A., Mould, A. P., Craig, S. E., Newham, P., Yamada, K. M., and Humphries, M. J. (2005). A specific alpha5beta1-integrin conformation promotes directional integrin translocation and fibronectin matrix formation. J. Cell Sci. *118*, 291–300.

Danen, E. H., Sonneveld, P., Brakebusch, C., Fassler, R., and Sonnenberg, A. (2002). The fibronectin-binding integrins alpha5beta1 and alphavbeta3 differentially modulate RhoA-GTP loading, organization of cell matrix adhesions, and fibronectin fibrillogenesis. J. Cell Biol. *159*, 1071–1086.

DeMali, K. A., Wennerberg, K., and Burridge, K. (2003). Integrin signaling to the actin cytoskeleton. Curr. Opin. Cell Biol. *15*, 572–582.

Dersch, P., and Isberg, R. R. (1999). A region of the *Yersinia pseudotuberculosis* invasin protein enhances integrin-mediated uptake into mammalian cells and promotes self-association. EMBO J. *18*, 1199–1213.

Essler, M., Linder, S., Schell, B., Hufner, K., Wiedemann, A., Randhahn, K., Staddon, J. M., and Aepfelbacher, M. (2003). Cytotoxic necrotizing factor 1 of *Escherichia coli* stimulates Rho/Rho-kinase-dependent myosin light-chain phosphorylation without inactivating myosin light-chain phosphatase in endothelial cells. Infect Immun. *71*, 5188–5193.

Fowler, T., Johansson, S., Wary, K. K., and Hook, M. (2003). Src kinase has a central role in in vitro cellular internalization of *Staphylococcus aureus*. Cell Microbiol. *5*, 417–426.

Fowler, T., Wann, E. R., Joh, D., Johansson, S., Foster, T. J., and Hook, M. (2000). Cellular invasion by *Staphylococcus aureus* involves a fibronectin bridge between the bacterial fibronectin-binding MSCRAMMs and host cell beta1 integrins. Eur. J. Cell Biol. *79*, 672–679.

Giannone, G., Dubin-Thaler, B. J., Dobereiner, H. G., Kieffer, N., Bresnick, A. R., and Sheetz, M. P. (2004). Periodic lamellipodial contractions correlate with rearward actin waves. Cell *116*, 431–443.

Greene, C., McDevitt, D., Francois, P., Vaudaux, P. E., Lew, D. P., and Foster, T. J. (1995). Adhesion properties of mutants of *Staphylococcus aureus* defective in fibronectin-binding proteins and studies on the expression of fnb genes. Mol. Microbiol. *17*, 1143–1152.

Hussain, M., Becker, K., von Eiff, C., Peters, G., and Herrmann, M. (2001). Analogs of Eap protein are conserved and prevalent in clinical *Staphylococcus aureus* isolates. Clin. Diagn. Lab. Immunol. *8*, 1271–1276.

Isberg, R. R., Hamburger, Z., and Dersch, P. (2000). Signaling and invasin-promoted uptake via integrin receptors. Microbes Infect. *2*, 793–801.

Jonsson, K., Signas, C., Muller, H. P., and Lindberg, M. (1991). Two different genes encode fibronectin-binding proteins in *Staphylococcus aureus*: the com-

plete nucleotide sequence and characterization of the second gene. Eur. J. Biochem. *202*, 1041–1048.

Jordens, I., Marsman, M., Kuijl, C., and Neefjes, J. (2005). Rab proteins, connecting transport and vesicle fusion. Traffic *6*, 1070–1077.

Katsumi, A., Orr, A. W., Tzima, E., and Schwartz, M. A. (2004). Integrins in mechanotransduction. J. Biol. Chem. *279*, 12001–12004.

Krut, O., Utermohlen, O., Schlossherr, X., and Kronke, M. (2003). Strain-specific association of cytotoxic activity and virulence of clinical *Staphylococcus aureus* isolates. Infect. Immun. *71*, 2716–2723.

Laschke, M. W., Kerdudou, S., Herrmann, M., and Menger, M. D. (2005). Intravital fluorescence microscopy: a novel tool for the study of the interaction of *Staphylococcus aureus* with the microvascular endothelium in vivo. J. Infect. Dis. *191*, 435–443.

Lo, S. H. (2004). Tensin. Int. J. Biochem. Cell Biol. *36*, 31–34.

Lowy, F. D. (1998). *Staphylococcus aureus* infections. N. Engl. J. Med. *339*, 520–532.

Massey, R. C., Kantzanou, M. N., Fowler, T., Day, N. P., Schofield, K., Wann, E. R., Berendt, A. R., Höök, M., and Peacock, S. J. (2001). Fibronectin-binding protein A of *Staphylococcus aureus* has multiple, substituting, binding regions that mediate adherence to fibronectin and invasion of endothelial cells. Cell Microbiol. *3*, 839–851.

May, R. C., and Machesky, L. M. (2001). Phagocytosis and the actin cytoskeleton. J. Cell Sci. *114*, 1061–1077.

McDevitt, D., Francois, P., Vaudaux, P., and Foster, T. J. (1994). Molecular characterization of the clumping factor (fibrinogen receptor) of *Staphylococcus aureus*. Mol. Microbiol. *11*, 237–248.

Menzies, B. E. (2003). The role of fibronectin binding proteins in the pathogenesis of *Staphylococcus aureus* infections. Curr. Opin. Infect. Dis. *16*, 225–229.

Miaczynska, M., Pelkmans, L., and Zerial, M. (2004). Not just a sink: endosomes in control of signal transduction. Curr. Opin. Cell Biol. *16*, 400–406.

Mould, A. P., and Humphries, M. J. (2004). Regulation of integrin function through conformational complexity: not simply a knee-jerk reaction? Curr. Opin. Cell Biol. *16*, 544–551.

Nishizaka, T., Shi, Q., and Sheetz, M. P. (2000). Position-dependent linkages of fibronectin-integrin-cytoskeleton. Proc. Natl. Acad. Sci. USA *97*, 692–697.

Nyberg, P., Sakai, T., Cho, K. H., Caparon, M. G., Fassler, R., and Bjorck, L. (2004). Interactions with fibronectin attenuate the virulence of *Streptococcus pyogenes*. EMBO J. *23*, 2166–2174.

Osiak, A. E., Zenner, G., and Linder, S. (2005). Subconfluent endothelial cells form podosomes downstream of cytokine and RhoGTPase signaling. Exp. Cell Res. *307*, 342–353.

Pankov, R., Cukierman, E., Katz, B. Z., Matsumoto, K., Lin, D. C., Lin, S., Hahn, C., and Yamada, K. M. (2000). Integrin dynamics and matrix assembly: tensin-dependent translocation of alpha(5)beta(1) integrins promotes early fibronectin fibrillogenesis. J. Cell Biol. *148*, 1075–1090.

Patti, J. M., *et al*. (1992). Molecular characterization and expression of a gene encoding a *Staphylococcus aureus* collagen adhesin. J. Biol. Chem. *267*, 4766–4772.

Que, Y. A., *et al*. (2005). Fibrinogen and fibronectin binding cooperate for valve infection and invasion in *Staphylococcus aureus* experimental endocarditis. J Exp. Med. *201*, 1627–1635.

Rasband, W. S. (2006). ImageJ. National Institutes of Health, Bethesda, MD. http://rsb.info.nih.gov/ij (1997–2006).

Schröder, A., Kland, R., Peschel, A., von Eiff, C., and Aepfelbacher, M. (2006). Live cell imaging of phagosome maturation in *Staphylococcus aureus* infected human endothelial cells: small colony variants are able to survive in lysosomes. Med. Microbiol. Immunol. *195*, 185–194. Epub 2006 April 5.

Schulte, R., Zumbihl, R., Kampik, D., Fauconnier, A., and Autenrieth, I. B. (1998). Wortmannin blocks *Yersinia* invasin-triggered internalization, but not interleukin-8 production by epithelial cells. Med. Microbiol. Immunol. *187*, 53–60.

Schwarz-Linek, U., Hook, M., and Potts, J. R. (2004). The molecular basis of fibronectin-mediated bacterial adherence to host cells. Mol. Microbiol. *52*, 631–641.

Scott, C. C., Dobson, W., Botelho, R. J., Coady-Osberg, N., Chavrier, P., Knecht, D. A., Heath, C., Stahl, P., and Grinstein, S. (2005). Phosphatidylinositol-4,5-bisphosphate hydrolysis directs actin remodeling during phagocytosis. J. Cell Biol. *169*, 139–149.

Sinha, B., Francois, P. P., Nusse, O., Foti, M., Hartford, O. M., Vaudaux, P., Foster, T. J., Lew, D. P., Herrmann, M., and Krause, K. H. (1999). Fibronectin-binding protein acts as *Staphylococcus aureus* invasin via fibronectin bridging to integrin alpha5beta1. Cell Microbiol. *1*, 101–117.

Sinha, B., Francois, P., Que, Y. A., Hussain, M., Heilmann, C., Moreillon, P., Lew, D., Krause, K. H., Peters, G., and Herrmann, M. (2000). Heterologously expressed *Staphylococcus aureus* fibronectin-binding proteins are sufficient for invasion of host cells. Infect. Immun. *68*, 6871–6878.

Sottile, J., and Chandler, J. (2005). Fibronectin matrix turnover occurs through a caveolin-1-dependent process. Mol. Biol. Cell *16*, 757–768.

Stevens, J. M., Galyov, E. E., and Stevens, M. P. (2006). Actin-dependent movement of bacterial pathogens. Nat. Rev. Microbiol. *4*, 91–101.

Welch, M. D., DePace, A. H., Verma, S., Iwamatsu, A., and Mitchison, T. J. (1997). The human Arp2/3 complex is composed of evolutionarily conserved subunits and is localized to cellular regions of dynamic actin filament assembly. J. Cell Biol. *138*, 375–384.

Wiedemann, A., Linder, S., Grassl, G., Albert, M., Autenrieth, I., and Aepfelbacher, M. (2001). *Yersinia enterocolitica* invasin triggers phagocytosis via beta1 integrins, CDC42Hs and WASp in macrophages. Cell Microbiol. *3*, 693–702.

Yam, P. T., and Theriot, J. A. (2004). Repeated cycles of rapid actin assembly and disassembly on epithelial cell phagosomes. Mol. Biol. Cell *15*, 5647–5658.

Zamir, E., and Geiger, B. (2001). Molecular complexity and dynamics of cell-matrix adhesions. J. Cell Sci. *114*, 3583–3590.

Zamir, E., *et al*. (2000). Dynamics and segregation of cell-matrix adhesions in cultured fibroblasts. Nat. Cell Biol. *2*, 191–196.